

XMM-Newton X-ray Observation of the High-Magnetic-Field Radio Pulsar PSR J1734–3333

S. A. Olausen¹, V. M. Kaspi¹, A. G. Lyne², & M. Kramer^{2,3}

ABSTRACT

Using observations made with the *XMM-Newton* Observatory, we report the probable X-ray detection of the high-magnetic-field radio pulsar PSR J1734–3333. This pulsar has an inferred surface dipole magnetic field of $B = 5.2 \times 10^{13}$ G, just below that of one anomalous X-ray pulsar (AXP). We find that the pulsar has an absorbed 0.5–2.0 keV flux of $(5\text{--}15) \times 10^{-15}$ erg s^{−1} cm^{−2} and that its X-ray luminosity L_X is well below its spin down luminosity \dot{E} , with $L_X < 0.1\dot{E}$. No pulsations were detected in these data although our derived upper limit is unconstraining. Like most of the other high- B pulsars, PSR J1734–3333 is X-ray faint with no sign of magnetar activity. We collect and tabulate the properties of this and all other known high- B radio pulsars with measured X-ray luminosities or luminosity upper limits and plot L_X versus B for them all.

Subject headings: pulsars: general — pulsars: individual (PSR J1734–3333) — stars: neutron — X-rays: stars

1. Introduction

Soft Gamma Repeaters (SGRs) and Anomalous X-ray Pulsars (AXPs) are now well accepted as being different though similar manifestations of “magnetars” — isolated neutron stars whose radiation is powered by their magnetic field (see Woods & Thompson 2006 or Mereghetti 2008 for a review). These objects are characterised by long spin periods (2–12 s), spin-down rates that, assuming conventional magnetic dipole braking, imply surface dipolar magnetic fields in the range $\sim 10^{14}\text{--}10^{15}$ G, X-ray luminosities of $10^{33}\text{--}10^{34}$ erg s^{−1} that are orders of magnitude greater than their spin-down luminosities, and great X-ray variability, ranging from short SGR-like bursts to major, slow-rise and long-lived X-ray flares (see Kaspi 2007 for a review). The bulk of SGR

¹Department of Physics, Rutherford Physics Building, McGill University, 3600 University Street, Montreal, Quebec, H3A 2T8, Canada

²Jodrell Bank Centre for Astrophysics, School of Physics and Astronomy, University of Manchester, Manchester, M13 9PL, UK

³MPI für Radioastronomie, Auf dem Hügel 69, 53121 Bonn, Germany

and AXP properties are well explained by the magnetar model (Thompson & Duncan 1995, 1996; Thompson et al. 2002).

However, there remain some outstanding challenges to the magnetar picture. Arguably the most important is the connection between magnetars and high-magnetic field radio pulsars. Some models predict that above the quantum critical field, $B_{QED} = 4.4 \times 10^{13}$ G, conventional radio emission should be suppressed. Yet there are now known over a half dozen otherwise ordinary radio pulsars having spin-down inferred magnetic field $B > 4 \times 10^{13}$ G (where $B = 3.2 \times 10^{19} (P\dot{P})^{1/2}$ G for a pulsar with period P and spin-down rate \dot{P}), with none showing evidence for conventional magnetar-like emission. Some, like PSRs J1847–0130 and J1718–3718, have B greater than those measured for *bona fide* magnetars, yet no anomalous X-ray emission (McLaughlin et al. 2003; Kaspi & McLaughlin 2005). Uncertainties in inferred B from spin-down can be substantial (e.g. Harding et al. 1999; Spitkovsky 2006), but still, in the magnetar picture, some evidence for anomalous X-ray emission is reasonably expected in some high- B radio pulsars. This is important overall for unifying the surprisingly varied manifestations of neutron stars into a physical framework (see Kaspi 2010 for a review).

Recently, the idea that high- B pulsars might exhibit anomalous X-ray emission was confirmed by the discovery of SGR-like X-ray bursts and a long-lived flux enhancement from what was previously thought to be a purely rotation-powered pulsar. Gavriil et al. (2008) found that the high- B pulsar PSR J1846–0258 at the center of the SNR Kes 75 emitted several SGR-like bursts in 2006, contemporaneous with a flux enhancement and a rotational glitch (see also Livingstone et al. 2010). This is the first pulsar that has quiescent X-ray luminosity that could be rotation-powered, and indeed has many properties of rotation-powered pulsars, while showing obvious magnetar-like behavior. Its small characteristic age of 884 yr lends further credence to the idea — PSR J1846–0258 could be a very young magnetar, and one of the “missing links” in the hypothesized high- B pulsar/magnetar evolutionary chain.

PSR J1734–3333 is a radio pulsar with $P = 1.169$ s and $\dot{P} = 2.3 \times 10^{-12}$, which imply a spin-down luminosity of $\dot{E} = 4\pi^2 I \dot{P} / P^3 = 5.6 \times 10^{34}$ ergs $^{-1}$ and a characteristic age of $\tau = P / 2\dot{P} = 8.1$ kyr. Its inferred surface dipolar magnetic field is $B = 5.2 \times 10^{13}$ G, which is among the highest of all known radio pulsars and just below those of *bona fide* magnetars such as 1E 2259+586 ($B = 5.9 \times 10^{13}$ G). Using 12 yr of phase-coherent radio timing observations at Jodrell Bank, this pulsar has had a stable braking index measured of $n = 1.0 \pm 0.3$ (Espinoza et al. 2010). At face value, this could imply that this high- B pulsar’s magnetic field is growing, i. e. its trajectory on a conventional P/\dot{P} diagram is up and to the right, towards the region occupied by the magnetars. This makes PSR J1734–3333 a good candidate for exhibiting magnetar-like anomalous X-ray emission. For this reason, we obtained *XMM-Newton* observations of this source which we report on here.

2. Observations and Results

One 10-ks observation of PSR J1734–3333 was carried out on 2009 March 9–10 using the *XMM-Newton* observatory (Jansen et al. 2001). The two EPIC MOS cameras (Turner et al. 2001) were operating in full-window mode with a time resolution of 2.7 s, and the EPIC pn camera (Strder et al. 2001) was in large-window mode providing a time resolution of 48 ms. For all three cameras the medium filter was in use. The total exposure time in this observation was 10.6 ks with each MOS camera and 8.7 ks with the pn.

The data were analyzed with the *XMM* Science Analysis System (SAS) version 8.0.0¹ with calibrations updated 2009 April 13. To identify times contaminated by strong background flaring that is sometimes present in *XMM* data, we extracted and examined light curves of photons above 10 keV over the entire field of view for the pn and MOS cameras. No flaring or significant background changes were found, so the entire exposure could be used in our analysis.

2.1. Imaging

In order to find a possible X-ray counterpart of PSR J1734–3333, we performed a blind search for point sources using the SAS tool `edetect_chain`.

A faint X-ray source was detected near the radio position of the pulsar by `edetect_chain` in all three cameras. In the pn camera it has 49 ± 10 counts in the 0.5–3.0 keV energy range and a likelihood ratio of $L_2 = -\ln P \simeq 29$ (where P is the probability that a random Poissonian fluctuation could produce the observed source counts). The source was also detected, in the same 0.5–3.0 keV energy band, in the MOS 1 camera with 21 ± 6 counts and $L_2 \simeq 12$ and in the MOS 2 camera with 31 ± 8 counts and $L_2 \simeq 17$. Outside this energy range there were no source counts detected.

Figure 1 shows the X-ray emission near the radio position of the pulsar, made by combining the pn, MOS 1, and MOS 2 images into a mosaic and smoothing with a Gaussian kernel of radius $\sigma = 3''$. The best-fit position of the X-ray source as reported by `edetect_chain` is (J2000) R.A. = $17^{\text{h}}34^{\text{m}}27^{\text{s}}.19 \pm 0^{\text{s}}.24$, DEC. = $-33^{\circ}33'22''.0 \pm 3''.0$, where these uncertainties consist of both the $1''$ statistical error and *XMM*'s absolute pointing uncertainty² of $2''$. In principle it is possible to reduce the pointing uncertainty by matching at least two bright X-ray sources in the field to known optical counterparts; unfortunately, the field of view of this observation contained only one such source.

The most up to date radio timing position for PSR J1734–3333 is R.A. = $17^{\text{h}}34^{\text{m}}26^{\text{s}}.9 \pm 0^{\text{s}}.2$,

¹See <http://xmm.esac.esa.int/sas/8.0.0/>

²See <http://xmm2.esac.esa.int/docs/documents/CAL-TN-0018.pdf>

DEC. = $-33^{\circ}33'20'' \pm 10''$ (Espinoza et al. 2010). The offset between the radio timing position and the centroid of the X-ray position in R.A. is $0^{\circ}29'$ or $\sim 0.9\sigma$, and is $2'0$ or $\sim 0.2\sigma$ in declination.

2.2. Spectroscopy

To obtain the X-ray spectrum, we extracted counts from the pn data using a circular region of $30''$ radius centered on the source. The background spectrum was taken from an elliptical annulus with semimajor and semiminor axes of $75''$ and $45''$ rotated 90° from north, surrounding but excluding the $30''$ source region. A response and ancillary response file were generated using the SAS tasks `rmfgen` and `arfgen`. The spectrum was grouped to have a minimum of 20 counts per bin with the `ftool grppha` and was fed into XSPEC 12.5.0ac for spectral fitting. We did not extract spectra from the MOS images due to the lower number of source counts in those cameras.

The X-ray spectrum was fit to absorbed power-law and absorbed blackbody models. Because of the small number of source counts, it was impossible to constrain the column density N_{H} . The Leiden/Argentine/Bonn and Dickey & Lockman Surveys of Galactic HI³ give the total column density along the line of sight to the pulsar as $N_{\text{H}} = (1.1 - 1.4) \times 10^{22} \text{ cm}^{-2}$, and from its dispersion measure of 578 pc cm^{-3} the distance to the pulsar is estimated to be 6.1 kpc with a $\sim 25\%$ uncertainty (Cordes & Lazio 2001). We therefore assumed an upper limit on N_{H} of $1.2 \times 10^{22} \text{ cm}^{-2}$, halved it to get a more reasonable estimate of $0.6 \times 10^{22} \text{ cm}^{-2}$ since, based on its distance, the pulsar is less than halfway through the Galaxy, and found best-fit models after fixing N_{H} to both values. The parameters of these best-fit models are shown in Table 1, and two of them are plotted in Figure 2. In general, a lower value of N_{H} corresponds to a power-law model with smaller photon index and a blackbody model with a higher kT .

2.3. Timing Analysis

The radio pulsar timing data were obtained using the Jodrell Bank 76-m Lovell telescope operating at a central observing frequency of around 1400 MHz, roughly contemporaneously with the X-ray observations. The TEMPO timing package⁴ was used to correct the times of arrival to the barycenter of the solar system assuming the position determined by Espinoza et al. (2010) and to fit a rotational model to these arrival times.

Based on this ephemeris for PSR J1734–3333, during the *XMM* observation the pulsar had an expected barycentric frequency of $854.9300124 \pm 0.0000004 \text{ mHz}$. Since the MOS cameras were operated in full-window mode with 2.7-s time resolution, their data cannot be used for our timing

³<http://cxc.harvard.edu/toolkit/colden.jsp>

⁴See <http://www.atnf.csiro.au/research/pulsar/tempo/>

analysis. A search for X-ray pulsations was done using the pn data after barycentering them using the SAS tool `barycen`. To do so, we extracted a total of 84 photon events in the 0.5–3.0 keV energy range from a region of $20''$ radius centered on the source. Although we used a smaller source region here than for the spectral analysis above in order to maximize the signal-to-noise, an identical background region was used for both the timing and spectral work. The aforementioned background region contained 286 events in the same energy band, implying there to be ~ 46 background photons in the source region. The source region event list was folded at the radio frequency using 16 phase bins, and the folded light curve was fit to a constant line. The best-fit χ^2 was 12.2 for 15 degrees of freedom, corresponding to a 67% probability that the folded curve could be produced from a data set containing no signal. Thus, no significant pulsations were detected. Searches were also conducted in the 0.5–10 keV and 1–2 keV energy bands with similar null results.

To find an upper limit for the pulsed fraction, we simulated event lists with the same number of total counts as found in the source region. The simulated signal had a sinusoidal profile with a random phase and had a user specified area pulsed fraction, where the area pulsed fraction is defined as the ratio of the pulsed part of the profile to the entire profile. However, given the expected number of background counts, even a signal with 100% area pulsed fraction could only be detected with $>3\sigma$ significance 5% of the time. Thus, we conclude that there are too few counts in our data set to set a meaningful upper limit on the pulsed fraction.

3. Discussion

Although the detected X-ray source is consistent with the radio timing position of PSR J1734–3333, given that no X-ray pulsations were detected from it at the radio period to provide unambiguous proof of association, it is reasonable to question whether the X-ray source really is associated with the radio pulsar. We can estimate the probability of a chance superposition from the $\log N$ – $\log S$ curves for *XMM-Newton* Galactic-plane sources in the 0.5–2.0 keV band (Motch 2006). Given the lowest reasonable value of absorbed flux in that band for the source, $\sim 5 \times 10^{-15}$ erg s $^{-1}$ cm $^{-2}$, the $\log N$ – $\log S$ curves predict ~ 180 sources per square degree at this flux or higher. The probability of a random X-ray source lying within the radio error ellipse, then, is only 0.1–0.3%.

On the other hand, looking at an optical image of the field of the *XMM* observation, there are several sources near the X-ray source. In fact, one of these optical sources (NOMAD Catalog ID 0564-0621454) lies within the X-ray error circle at coordinates R.A. = $17^{\text{h}}34^{\text{m}}27^{\text{s}}.319 \pm 0^{\text{s}}.008$, DEC. = $-33^{\circ}33'22''.61 \pm 0''.05$. Therefore the possibility must be considered that the X-ray source is associated with this optical source in addition to or instead of the radio pulsar.

Assuming that the X-ray source is associated with 0564-0621454, its X-ray to optical flux ratio can be estimated using the following formula from Georgakakis et al. (2004):

$$\log (f_{\text{X}}/f_{\text{opt}}) = \log f (0.5\text{--}8 \text{ keV}) + 0.4B + 4.89.$$

Here f (0.5–8 keV) is the unabsorbed X-ray flux in that energy band and $B = 18.79$ is the optical magnitude of 0564-0621454 taken from the USNO-B1.0 catalog. Although the unabsorbed X-ray flux is even less constrained than the absorbed flux used above, we can calculate a rough upper limit of $\log(f_X/f_{\text{opt}}) < 1$. PSR J1734–3333 is an isolated neutron star, however, which typically has $\log(f_X/f_{\text{opt}}) \sim 5$ (Treves et al. 2000; Kaspi et al. 2006). Therefore, we conclude that if our X-ray source is associated with 0564-0621454, it cannot also be associated with PSR J1734–3333, and vice versa.

Finally, just as the probability of a chance superposition of an X-ray source with the pulsar’s radio position was estimated above, it is a simple matter to calculate the probability of an optical source coinciding with the X-ray position. A query of the USNO-B1.0 catalog returns almost 5500 sources within a $10'$ radius of the centre of the *XMM* field. The probability of one of these sources lying within the $3''$ X-ray error circle by chance is $\sim 12\%$, much higher than the probability of a chance X-ray/radio alignment. Even accounting for the fact that 0564-0621454 is only $2''$ away from the X-ray position, the probability of a chance superposition is still 5–6%. We conclude that it is highly likely that the X-ray source is associated with PSR J1734–3333, and much less probable that it is associated with the optical source 0564-0621454.

With so few source counts to work with, the pulsar’s spectrum allows for such a wide range of possible photon indices and blackbody temperatures that it is impossible to eliminate a thermal or non-thermal source for the X-ray emission. Among the four models shown in Table 1, the absorbed 0.5–2.0 keV flux is relatively well constrained, to within a factor of 2–3. However, since assuming a higher value of N_{H} yields a steeper power-law index or a lower kT , the unabsorbed 0.5–2.0 keV flux is much less constrained and varies by nearly 2 orders of magnitude within and between the models. Assuming a distance to the pulsar of 6.1 kpc as estimated from the dispersion measure, the 0.5–10.0 keV X-ray luminosity of PSR J1734–3333 is in the range $1\text{--}34 \times 10^{32} \text{ erg s}^{-1}$. However, $L_X < \dot{E}$ for all these models, even allowing for a 25% uncertainty in the estimated distance, with $L_X/\dot{E} \sim 0.1\text{--}10\%$. Furthermore, the high end of the luminosity range corresponds to the high N_{H} models, suggesting that the pulsar’s true X-ray luminosity more likely lies in the lower end of the range.

In Table 2 we list all high-magnetic field radio pulsars with inferred magnetic field $B > B_{\text{QED}}$, as well as several others with $B > 1.5 \times 10^{13} \text{ G}$, that have measured X-ray luminosities or luminosity upper limits. Of these stars only one, PSR J1846–0258, has exhibited clear magnetar-like behavior (Gavriil et al. 2008). Other than that, high- B pulsars show spectral properties that are much different from active magnetars, being much softer and fainter X-ray sources. They do, however, show some similarities with transient magnetars, which in quiescence are also softer, fainter X-ray sources. One transient magnetar in particular, XTE J1810–197, displayed spectral properties in quiescence that were consistent with those of the detected high- B pulsars ($kT \approx 0.18 \text{ keV}$ and 0.5–10 keV $L_X \sim 7 \times 10^{32} \text{ erg s}^{-1}$) (Gotthelf et al. 2004).

Additionally, we took the reported X-ray luminosities for the pulsars in Table 2, extrapolated

them to the 0.5–10 keV energy band, and plotted this value versus inferred magnetic field in Figure 3. The resulting plot does show evidence of a correlation between the two quantities, with higher B -field stars having higher 0.5–10 keV L_X ; certainly the pulsars here with $B \gtrsim 4 \times 10^{13}$ G are brighter in X-rays than those with $B \lesssim 4 \times 10^{13}$ G. There are some caveats that should be noted, however. In particular, of the four pulsars with the highest B fields, two have only X-ray luminosity upper limits and the other two have only weak detections with poorly constrained luminosity measurements. Future observations may show some or all of these pulsars to be substantially more X-ray dim than PSR J1119–6127 or PSR J1819–1458, which would considerably weaken the possible correlation.

Although the spectrum of PSR J1734–3333 is poorly constrained, it is evident that it has much more in common with the other high- B pulsars than with the magnetars. Most magnetars, even in quiescence, have X-ray luminosities exceeding their spin-down luminosities by orders of magnitude; for this pulsar, as with the other high- B radio pulsars, the opposite is true. In particular, its 2–10 keV X-ray luminosity is well below that of any known magnetar (see Woods & Thompson 2006, Table 14.1). Therefore, while PSR J1734–3333 may be evolving towards the rotational properties of a magnetar (Espinoza et al. 2010), it currently retains essentially the radiative properties of a radio pulsar. What is less clear from these data, however, is whether its 0.5–10 keV L_X/\dot{E} is similar to or greater than that of PSR J1846–0258 in quiescence (~ 1 –10%), or whether it is considerably smaller as with most other high- B pulsars. Unfortunately, due to the poor statistics it is difficult to compare the spectrum of PSR J1734–3333 with those of other high- B pulsars and magnetars. Longer X-ray observations are needed in the future to better constrain the luminosity, obtain a good spectrum, and search for X-ray pulsations.

We thank M. Livingstone for useful comments. V.M.K. receives support from NSERC, FQRNT, CIFAR, and holds a Canada Research Chair and the Lorne Trottier Chair in Astrophysics and Cosmology.

REFERENCES

- Caswell, J. L., McClure-Griffiths, N. M., & Cheung, M. C. M. 2004, MNRAS, 352, 1405
- Cordes, J. M., & Lazio, T. J. W. 2001, ApJ, 549, 997
- Espinoza, C. M., Lyne, A. G., Kramer, M., Manchester, R. N., & Kaspi, V. M. 2010, Nature, submitted
- Gavriil, F. P., Gonzalez, M. E., Gotthelf, E. V., Kaspi, V. M., Livingstone, M. A., Woods, P. M. 2008, Science, 319, 1802
- Georgakakis, A., et al. 2004, MNRAS, 349, 135
- Gonzalez, M. E., Kaspi, V. M., Lyne, A. G., & Pivovarov, M. J. 2004, ApJ, 610, L37

- Gotthelf, E. V., Halpern, J. P., Buxton, M., & Bailyn, C. 2004, *ApJ*, 605, 368
- Harding, A. K., Contopoulos, I., & Kazanas, D. 1999, *ApJ*, 525, L125
- Jansen, F., et al. 2001, *A&A*, 365, L1
- Kaplan, D. L., Esposito, P., Chatterjee, S., Possenti, A., McLaughlin, M. A., Camilo, F., Chakrabarty, D., & Slane, P. O. 2009, *MNRAS*, 400, 1445
- Kaspi, V. M. 2007, *Ap&SS*, 308, 1
- Kaspi, V. M. 2010, *PNAS*, 107, 7147
- Kaspi, V. M., & McLaughlin, M. A. 2005, *ApJ*, 618, L41
- Kaspi, V. M., Roberts, M. S. E., & Harding, A. K. 2006, in *Compact Stellar X-ray Sources*, ed. W. H. G. Lewin & M. van der Klis (Cambridge: Cambridge Univ. Press)
- Leahy, D. A., & Tian, W. W. 2008, *A&A*, 480, L25
- Livingstone, M. A., Kaspi, V. M., & Gavriil, F. P. 2010, *ApJ*, 710, 1710
- McLaughlin, M. A., et al. 2003, *ApJ*, 591, L135
- McLaughlin, M. A., et al. 2007, *ApJ*, 670, 1307
- Mereghetti, S. 2008, *A&A Rev.*, 15, 225
- Motch, C. 2006, in *ESA Special Publication, Vol. 604, The X-ray Universe 2005*, ed. A. Wilson, 38
- Ng, C.-Y., Slane, P. O., Gaensler, B. M., & Hughes, J. P. 2008, *ApJ*, 686, 508
- Pivovarov, M. J., Kaspi, V. M., & Camilo, F. 2000, *ApJ*, 535, 379
- Reynolds, S. P., et al. 2006, *ApJ*, 639, L71
- Safi-Harb, S., & Kumar, H. S. 2008, *ApJ*, 648, 532
- Strder, L., et al. 2001, *A&A*, 365, L18
- Spitkovsky, A. 2006, *ApJ*, 648, L51
- Thompson, C., & Duncan, R. C. 1995, *MNRAS*, 275, 255
- Thompson, C., & Duncan, R. C. 1995, *ApJ*, 473, 322
- Thompson, C., Lyutikov, M., & Kulkarni, S. R. 2002, *ApJ*, 574, 332
- Treves, A., Turolla, R., Zane, S., & Colpi, M. 2000, *PASP*, 112, 297

Turner, M. J. L., et al. 2001, *A&A*, L27

Woods, P. M., & Thompson, C. 2006, in *Compact Stellar X-ray Sources*, ed. W. H. G. Lewin & M. van der Klis (Cambridge: Cambridge Univ. Press)

Zhu, W., Kaspi, V. M., Gonzalez, M. E., & Lyne, A. G. 2009, *ApJ*, 704, 1321

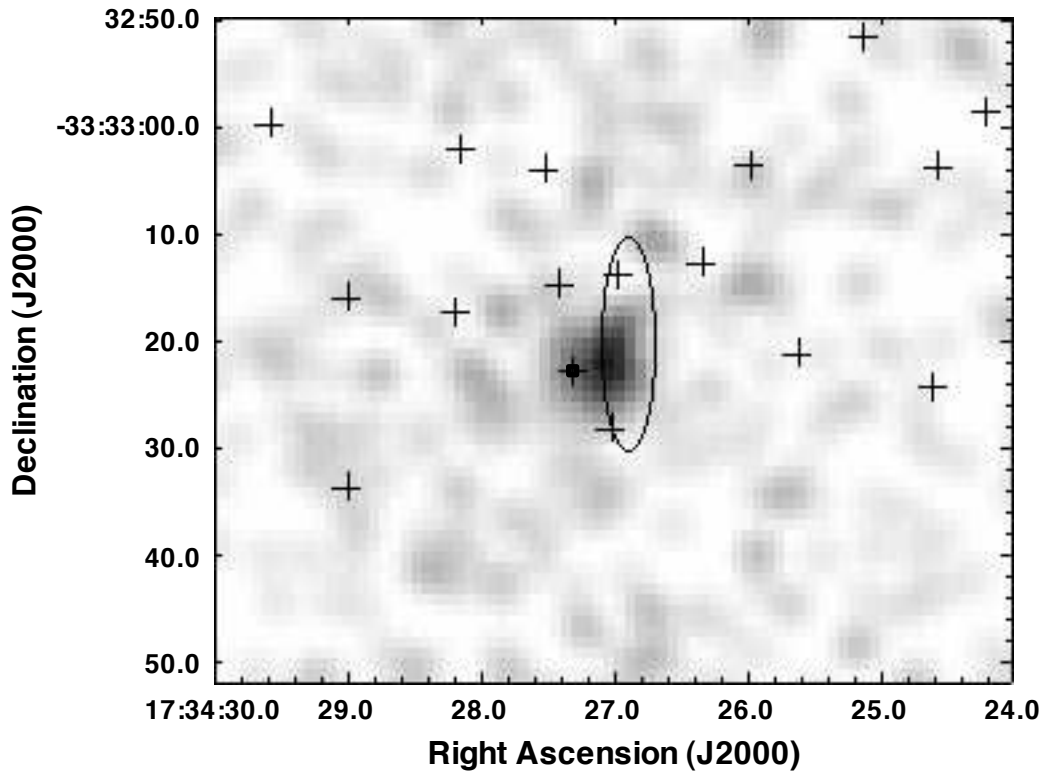


Fig. 1.— *XMM* image of the PSR J1734–3333 field in the 0.5 – 3.0 keV band, smoothed by a Gaussian kernel with $\sigma = 3''$. The radio timing position is shown by the ellipse, and the crosses denote the positions of optical sources from the USNO-B1.0 catalog. The optical source closest to the X-ray source (NOMAD Catalogue ID 0564-0621454) is represented by the cross marked with a box.

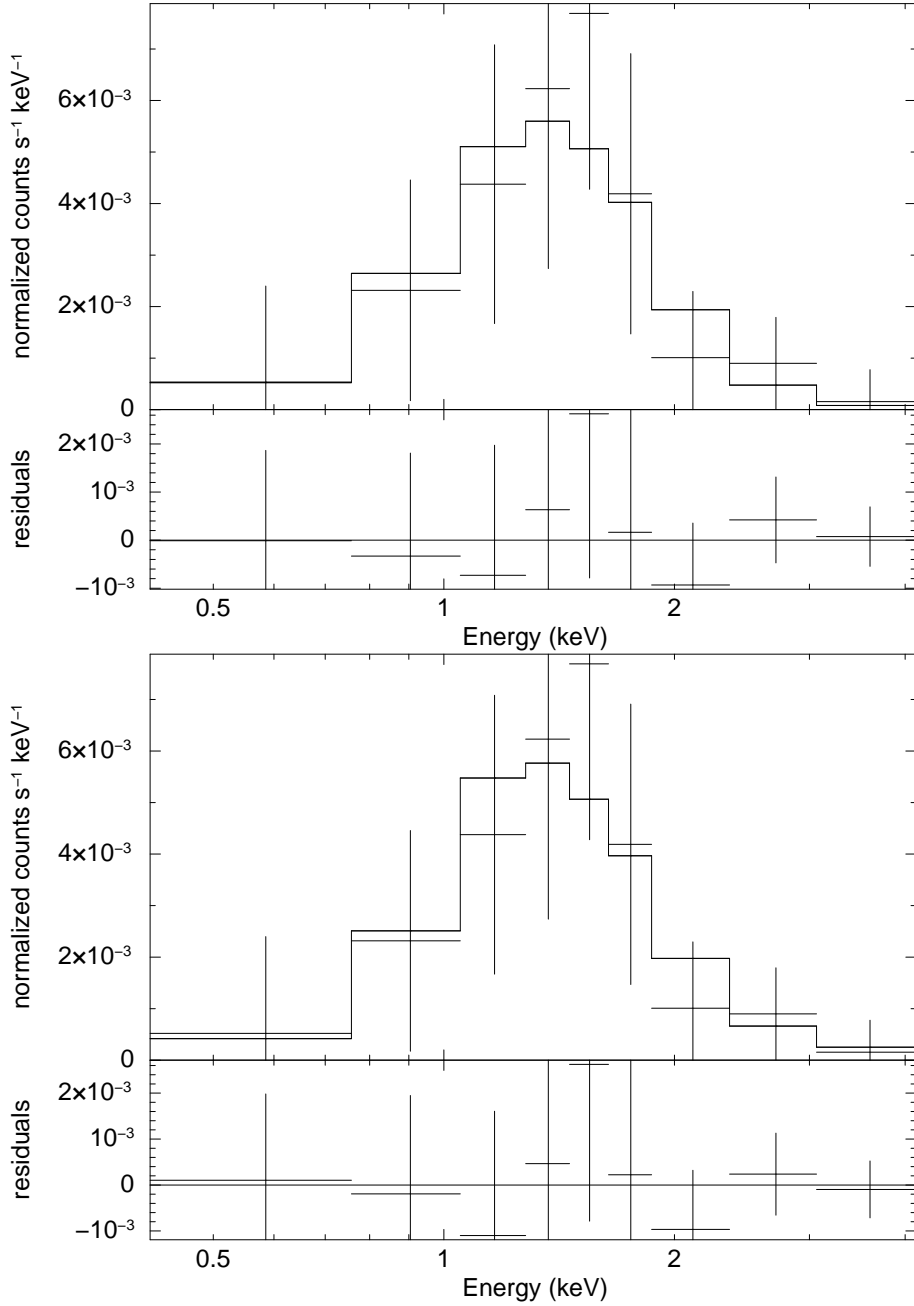


Fig. 2.— *XMM* pn spectrum of the possible X-ray counterpart to PSR J1734–3333. The spectrum is binned to contain a minimum of 20 counts per bin. Top: Best-fit blackbody model for fixed $N_{\text{H}} = 6.0 \times 10^{21} \text{ cm}^{-2}$. Bottom: Best-fit power-law model for fixed $N_{\text{H}} = 1.2 \times 10^{22} \text{ cm}^{-2}$.

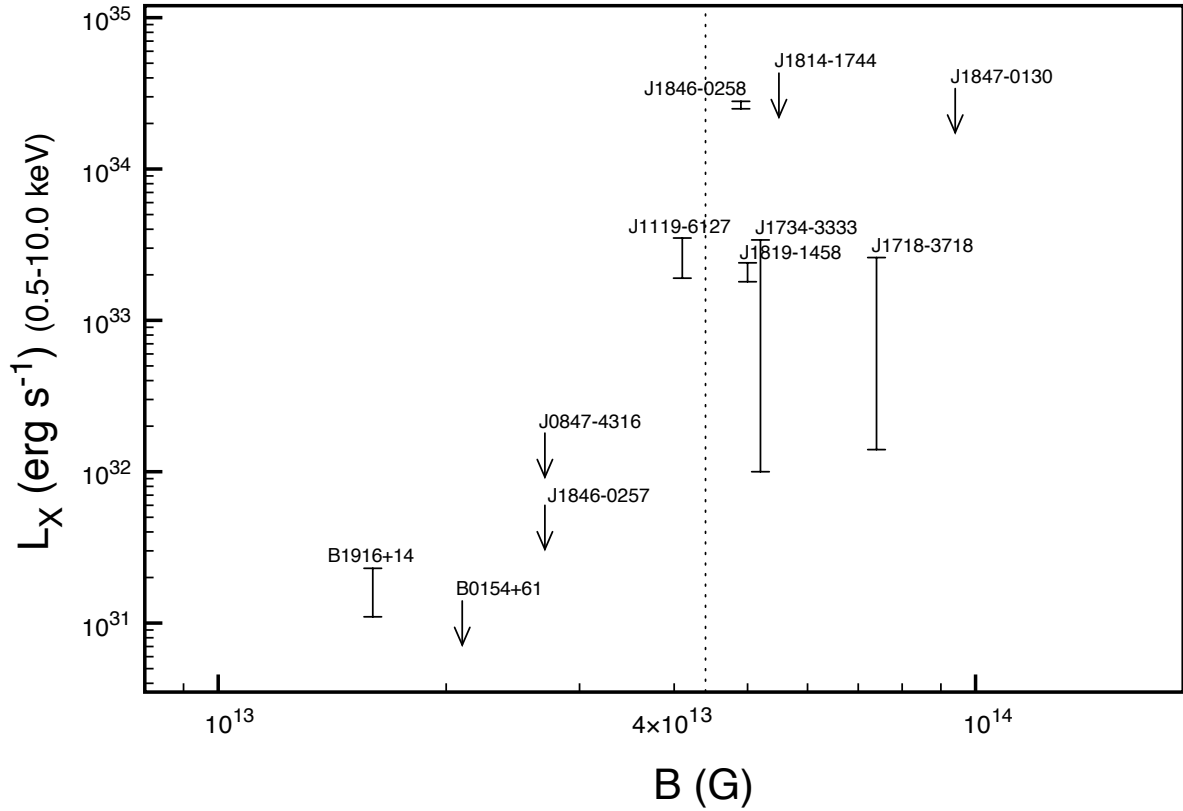


Fig. 3.— X-ray luminosity (0.5–10 keV) versus magnetic field strength for X-ray observed high- B radio pulsars. Luminosity values from the original references were extrapolated to this energy band based on the fit or assumed spectral model. Note that the value plotted for PSR J1846–0258 is its quiescent X-ray luminosity. The dotted line represents the quantum critical field, $B_{QED} = 4.4 \times 10^{13}$ G. See Table 2 for references.

Table 1. Spectral Parameters for PSR J1734–3333

Parameter	Power Law		Blackbody	
N_H (10^{22} cm $^{-2}$)	1.2	0.6	1.2	0.6
Γ^a	$4.2^{+1.8}_{-1.4}$	$2.6^{+1.3}_{-1.0}$
kT (keV) ^a	$0.25^{+0.13}_{-0.08}$	$0.34^{+0.19}_{-0.11}$
χ^2 (dof)	1.44(7)	2.55(7)	1.35(7)	1.49(7)
f_{abs} (10^{-15} erg s $^{-1}$ cm $^{-2}$) ^b	6.4–16	5.8–15	5.7–15	6.1–15
f_{unabs} (10^{-14} erg s $^{-1}$ cm $^{-2}$) ^c	6.7–77	1.7–7.5	3.6–21	1.5–4.9

^aUncertainty ranges indicate 90% confidence intervals.

^bAbsorbed flux in the 0.5–2.0 keV band. Range indicates 90% confidence interval.

^cUnabsorbed flux in the 0.5–2.0 keV band. Range indicates 90% confidence interval.

Table 2. High-Magnetic-Field Radio Pulsars

Name	P (s)	B (10^{13} G)	\dot{E} (erg s^{-1})	τ (kyr)	d^a (kpc)	L_X (erg s^{-1})	Energy range (keV)	Reference
J1847–0130	6.71	9.4	1.7×10^{32}	83	8.4	$< 5 \times 10^{33}$	2–10	McLaughlin et al. (2003)
J1718–3718	3.38	7.4	1.6×10^{33}	34	4.5	$0.2\text{--}6 \times 10^{33}$	bolometric	Kaspi & McLaughlin (2005)
J1814–1744	3.98	5.5	4.7×10^{32}	85	10	$< 6.3 \times 10^{35}$	0.1–2.4	Pivovarov et al. (2000)
J1734–3333	1.17	5.2	5.6×10^{34}	8.1	6.1	$< 4.3 \times 10^{33}$	2–10	This work
						$0.1\text{--}3.4 \times 10^{33}$	0.5–10	
J1819–1458 ^b	4.26	5.0	2.9×10^{32}	117	3.6	$2.8\text{--}4.3 \times 10^{33}$	0.3–5	McLaughlin et al. (2007)
J1846–0258	0.33	4.9	8.1×10^{36}	0.9	6.0 ^c	$2.5\text{--}2.8 \times 10^{34e}$	0.5–10	Ng et al. (2008)
						$1.2\text{--}1.7 \times 10^{35f}$	0.5–10	Ng et al. (2008)
J1119–6127	0.41	4.1	2.3×10^{36}	1.7	8.4 ^d	$1.9\text{--}3.2 \times 10^{33}$	0.5–7	Safi-Harb & Kumar (2008)
J0847–4316 ^b	5.98	2.7	2.2×10^{31}	790	3.4	$< 1 \times 10^{32}$	0.3–8	Kaplan et al. (2009)
J1846–0257 ^b	4.48	2.7	7.1×10^{31}	442	5.2	$< 3 \times 10^{32}$	0.3–8	Kaplan et al. (2009)
B0154+61	2.35	2.1	5.7×10^{32}	197	1.7	$< 8 \times 10^{31}$	0.3–10	Gonzalez et al. (2004)
B1916+14	1.18	1.6	5.1×10^{33}	88	2.1	$\sim 3 \times 10^{31}$	bolometric	Zhu et al. (2009)

^aUnless otherwise noted, all distances were estimated from the dispersion measure of the source.

^bPulsar classified as a rotating radio transient (RRAT).

^cThe distance to PSR J1846–0258 was found from H I and ^{13}CO spectral measurements (Leahy & Tian 2008).

^dThe distance to PSR J1119–6127 was found from H I absorption measurements (Caswell et al. 2004).

^eThis value is from 2000, prior to this pulsar’s 2006 outburst.

^fThis value is from 2006, during this pulsar’s 2006 outburst.